THE PENNSYLVANIA STATE UNIVERSITY
SCHREYER HONORS COLLEGE

DEPARTMENT OF BIOMEDICAL ENGINEERING

INVESTIGATING THE EFFICACY OF CAR T-CELLS EXPRESSING TQM-13 IN TARGETING GLIOBLASTOMA

HALI JIANG
SPRING 2019

A thesis
submitted in partial fulfillment
of the requirements
for a baccalaureate degree
in Biomedical Engineering
with honors in Biomedical Engineering

Reviewed and approved* by the following:

Cheng Dong
Distinguished Professor and Department Head of Biomedical Engineering
Thesis Supervisor

Justin Brown
Associate Professor and Coordinator of the Undergraduate Program
Honors Adviser

Xiaojun (Lance) Lian
Assistant Professor of Biology and Biomedical Engineering
Faculty Reader

* Signatures are on file in the Schreyer Honors College.

ABSTRACT

Chimeric antigen receptor (CAR) modified T-cell therapy has proven to be an attractive immunotherapy that involves the genetic modification of T-lymphocytes to target specific antigens expressed by cancer cells. Recent research has shown promising results for CAR T-cells expressing Targeted Quadruple Mutant-13 (TQM-13), a mutant version of interleukin-13 (IL-13), in targeting and attacking glioblastoma multiforme (GBM). CAR T immunotherapy is able to utilize the inherent ability of T-lymphocyte cells to migrate across the blood-brain barrier (BBB), a specialized, highly selective, semipermeable membrane formed by neurovascular endothelial cells that restrict the substances that enter and exit the central nervous system. Additionally, the CAR modification leads to specialized targeting of a specific antigen displayed by the tumor of interest. Once attached and bound to the target, the CAR T-cell becomes activated leading to T-cell proliferation, secretion of apoptosis-inducing proteins, and subsequent destruction of the tumor cells. The present study examines the ability of CAR T-cells expressing TQM-13 to target GBM. The results indicate that CAR modification did not impede the cells' natural ability to form intercellular gaps nor their ability to extravasate through an endothelial layer, both crucial steps in crossing the BBB. Additionally, it was found that CAR modification significantly increased both the total number of adhesions observed as well as the length of time the CAR T-cells adhered to GBM cells under flow conditions. These results imply that a TQM-13 directed CAR design has the potential to be a powerful therapeutic tool in the treatment of GBM.

TABLE OF CONTENTS

LIST OF FIGURES

ACKNOWLEDGEMENTS

First and foremost, I would like to express my sincere gratitude to my advisor, Dr. Cheng Dong, for sharing his expertise and guidance throughout this process. Additionally, I would like to thank Dr. Virginia Sanabria for taking me under her wing and sharing her knowledge, advice, and support. I would also like to thank Josh Reynolds for his unfaltering help and encouragement throughout this project, and for being so open to assisting me in the completion of my work. Finally, I would like to thank my friends and family for their continued love and confidence in me. I especially want to thank Derek McBlane, Sarah Chomos, and Josh Reynolds for volunteering to donate blood for my experimentation. This thesis, and my tremendous growth as a researcher and student would not have been possible without them.

Chapter 1

Introduction

1.1 Motivation and Background

An estimated 700,000 Americans today are living with a primary brain tumor, with 80% of malignant brain tumors being classified as gliomas [1]. Glioblastoma multiforme (GBM) is a Grade IV glioma tumor, the most aggressive and most common primary brain tumor. Currently, brain tumor treatment varies on a case-to-case basis depending on multiple patient factors, with the main treatments being surgical resection, radiation therapy, and chemotherapy [2]. Usually a patient will undergo a combination of these treatments, but even after treatment, the median survival rate for adults is still only 11-15 months [3].

Immunotherapies have emerged as an exciting new cancer treatment due to strong preliminary findings, as well as the appeal of employing the patient's own immune system to fight cancer cells. The biggest advantages of immunotherapy are its adaptability, high specificity targeting, low invasiveness and toxicity, and durability [4]. The creation of an effective immunotherapy method targeting GBM will greatly improve patients' quality of life and life expectancy. One especially promising method of immunotherapy is the use of chimeric antigen receptor (CAR) T-cell therapy.

1.1.1 The Blood-Brain Barrier

One of the main obstacles in developing a treatment to target GBM is the presence of the blood-brain barrier (BBB). This endothelial cell layer is highly selective and prevents the transport of bacteria, large molecules, and most small molecules into the brain [5]. Consequently, the BBB prevents the entry of harmful compounds, but also makes it difficult to ensure that a treatment will be effective, as it may be unable to reach the tumor site.

The endothelial cells making up the BBB lack fenestration, have few pinocytotic vesicles, and have extensive tight junctions [5]. The combination of these key characteristics limits the movement of substances past the BBB. In addition to a layer of brain endothelial cells, pericytes, astrocytes, microglia, and structural proteins (e.g. collagen and laminin) are present within the BBB [6]. A figure illustrating the anatomy of the BBB is included below in **Figure 1**. Pericytes form the first layer surrounding the brain endothelial cells and are found at a ratio of 1:3 to the endothelial cells. They function to regulate the diameter of the capillaries, controlling blood flow, and are crucial in monitoring tissue survival within the BBB. Astrocytes work to ensure that a homeostasis of ion, water, and metabolites concentrations is maintained with the extracellular environment. They also interact closely with neurons to determine plasticity and regulate neurotransmitters [7].

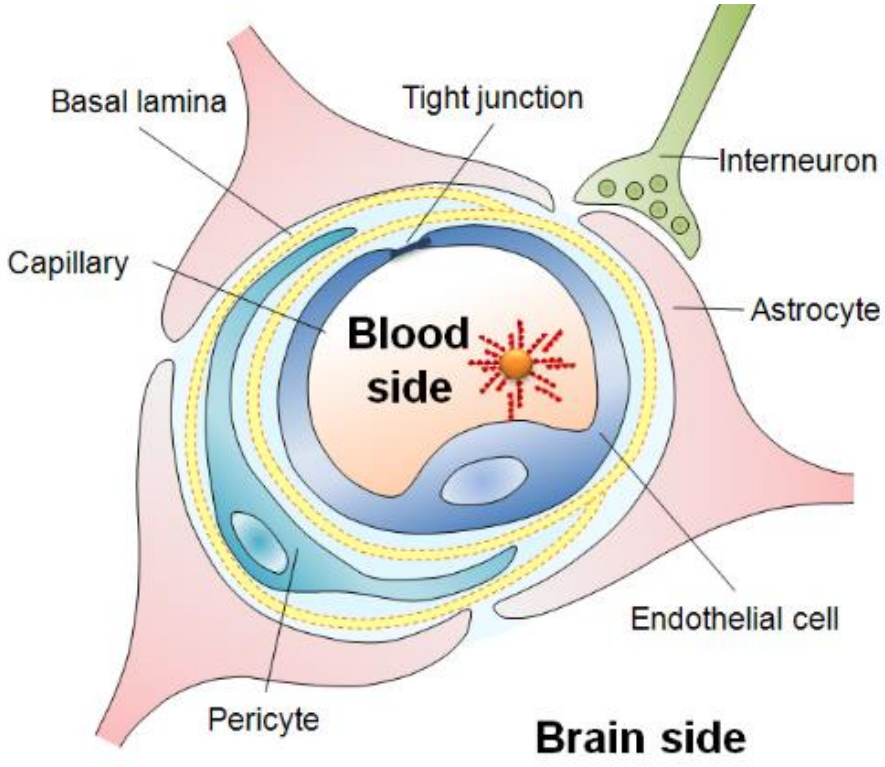

Figure 1: Schematic of the different components involved in the blood-brain-barrier [8].

Under normal circumstances, due to the functionality of the cells that compose the BBB, permeability is severely restricted. This high selectivity is important in protecting the brain from pathogens, but also makes it difficult for treatments to cross. Drugs that are able to make it through the BBB undergo transmembrane diffusion and have a low molecular weight (less than 400 Da) and a high lipid solubility [9]. In the case of GBM, most chemotherapeutics cannot cross the BBB and are usually transported out of cells by multidrug transporters [6].

However, it has been confirmed that freshly activated T-lymphocytes are able to open and migrate across the BBB. They do so by interacting with the central nervous system neurovasculature and are involved in the regulation of the BBB when infection, injury, or disease are present [10]. In fact, once the migration of T-cells begins, the permeability of the BBB

increases, favoring further migration of T-cells [11]. These facts support the promising method of using T-lymphocytes in immunotherapies targeting GBM.

The *in vitro* model of the BBB employed in the following experiments is only composed of endothelial cells, lacking the other components of the neurovascular unit described above and illustrated in **Figure 1**. Although the model used is simplified, it focuses on the endothelial cells, the first layer of the BBB. Results obtained from this model will provide valuable preliminary data predicting the results that would be observed in an *in vivo* model. Since human brain microvascular endothelial cells (HBMVEC) are known to be unreliable and hard to acquire [12], bovine brain microvascular endothelial cells (BBMVEC) were chosen as a substitute due to characteristics that closely mimic those of HBMVEC cells including: the presence of tight junctions, monoamine oxidase activity, and low levels of pinocytotic vesicles [13].

1.1.2 CAR T-Cell Therapy

CAR T-cell immunotherapy involves the collection and genetic modification of the patient's T-lymphocytes to express a CAR receptor that targets a specific antigen found on the patient's tumor. Once the CAR T-cells successfully bind to the target tumor cells they become activated and begin proliferating, transforming into cytotoxic T-lymphocytes [14]. The process of creating and administrating CAR T-cells is illustrated below in **Figure 2**.

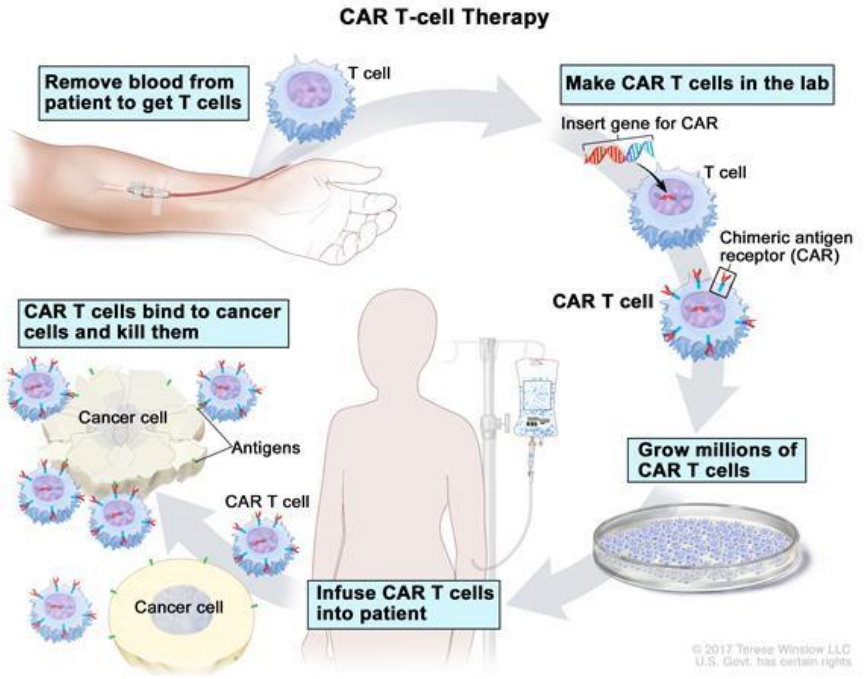

Figure 2: Process of creation and administration of CAR T-cells to patient [16].

The main components of the CAR design include the ectodomain, hinge, and transmembrane domain. The ectodomain is most commonly a single chain variable fragment (scFv), but can also be composed of modifications of a receptor or molecule. The ectodomain serves to target the specific tumor antigen and ensures specificity. The hinge region design allows for variability in the flexibility and length of the CAR and is located between the ectodomain and the transmembrane domain. Finally, the transmembrane domain is typically obtained from CD3-ζ, CD4, CD8, or CD28 molecules. Each of these molecules provide different characteristics and interactions, affecting the behavior of the T-lymphocyte [15].

Currently, there are two CAR T-cell therapies approved for use by the FDA for applications in B-cell non-Hodgkin's lymphoma and childhood acute lymphoblastic leukemia [17]. Using CAR T therapy to treat solid tumors, such as GBM, faces several hurdles including the selection of a target antigen that is homogeneously expressed by the tumor cells, the

immunosuppressive tumor microenvironment, and difficulty facing T-lymphocytes in infiltrating the solid tumor [18].

Despite these obstacles, recent research has shown promise for CAR T-cells targeting IL-13α2 for application in GBM. Approximately 75% of GBM cells show elevated expression of IL-13α2, and its expression is absent in healthy brain cells and most other organs with the exception of the testes [19], [20]. Some clinical studies have already been completed utilizing CAR designs involving derivatives of the wildtype IL-13 to target IL-13α2, with most showing promising results. One study injected the CAR T-cells intracranially to patients, leading to complete elimination of GBM tumors that continued for 7.5 months after the CAR T transfer with no recurrence of the treated tumors [21].

1.1.3 TQM-13 CAR Design

In spite of these promising results, one concern with the use of derivatives of the wildtype IL-13 is its nonspecific binding to the target antigen IL13Rα2. The wildtype IL-13 and its derivative can also bind to the IL13Rα1/IL4Rα heterodimer, which is readily expressed in normal brain and tissue cells. A mutated version of IL-13, the targeted quadruple mutant-13 (TQM-13) involves mutations of four amino acids found in wildtype IL-13. TQM-13 has shown increased specificity for IL13Rα2, with reduced affinity towards IL13Rα1/IL4Rα [19], indicating higher specificity in targeting GBM.

1.2 Objectives

There were three main objectives of this thesis with an overall goal of comparing the effectiveness of CAR T modified lymphocytes expressing TQM-13 in targeting GBM when compared to the control group of non-modified lymphocytes. The first objective was to analyze the ability of CAR T-cells to statically open intercellular gaps within the BBB. This objective provides preliminary data investigating the ability of the CAR T-cells to begin the first steps of cell extravasation through the endothelial layer. The second objective analyzed the ability of CAR T-cells to migrate across the BBB. The added flow component in this objective creates an environment mimicking physiological conditions of blood flow across the BBB in an attempt to simulate the entire extravasation process. The combination of the first two objectives provides insight into the ability of CAR T-cells to combat one of the biggest complications facing brain tumor therapies: overcoming the BBB. Finally, the third objective was to quantify the binding strength between CAR T-cells and the target GBM cells. This objective gives valuable information on the ability of the selected TQM-13 CAR molecule in targeting and successfully binding to GBM cells, predicting the likelihood of *in vivo* success.

1.3 Thesis Organization

This thesis is comprised of seven different chapters. The first introduces the problem and an explanation of relevant biology. Chapter 2 details the materials and methods used to carry out each experiment conducted for this thesis. Chapter 3 summarizes results of the T-lymphocyte separation from whole blood samples and the infection process of the lymphocytes with the CAR receptor. Chapter 4 summarizes the results from the static intercellular gap opening experiments,

Chapter 5 describes the results from the flow extravasation experiments, and Chapter 6 speaks to the results from the binding strength experiments. Finally, Chapter 7 concludes the thesis with a summary of the results and a discussion of possible future work.

Chapter 2

Materials and Methods

2.1 Cell Culture Protocols

Bovine brain microvascular endothelial cells (BBMVEC) (Cell Applications, San Diego, CA), human glioblastoma multiforme (GBM) cells expressing a luciferase reporter (U87-LUC), (Perkins Elmer, Waltham, MA), and primary T-lymphocytes separated from whole human blood were utilized. All cell types were grown in treated polystyrene Petri dishes and incubated at 37°C and 5% CO_2.

2.1.1 BBMVEC Cell Culture Protocol

BBMVEC cells were cultured in bovine brain endothelial growth medium (Cell Applications, San Diego, CA) with 2% penicillin streptomycin (Corning, Manassas, VA). Petri dishes used for the culture of these cells were pre-treated with 2 mL of attachment factor solution (Cell Applications, San Diego, CA) for at least 30 minutes before the addition of cells. When BBMVEC cells were confluent, the media in the Petri dish was aspirated and the cells were washed with 5 mL of Dulbecco's modified phosphate buffer saline (DPBS). After washing, the DPBS was aspirated, 1 mL of 0.25% trypsin-EDTA (Gibco, Grand Island, NY) was added, and the plate was incubated at 37°C for 5 minutes to allow for cell detachment. 3 mL of media was then added to the cells and this cell suspension was centrifuged at 1500 RPM for 5 minutes at

15°C. The resulting supernatant was aspirated and the cells were resuspended in media to be passaged or seeded for an experiment.

2.1.2 U87-LUC Cell Culture Protocol

U87-LUC cells were cultured in minimum essential media (MEM) (Corning, Manassas, VA) with 10% fetal bovine serum (FBS) (Atlanta Biologicals, Flowery Branch, GA) and 2% penicillin streptomycin. The protocol for culturing of these cells is identical to that of BBMVEC cells with the exception of attachment factor solution Petri dish pretreatment.

2.1.3 Lymphocyte Cell Culture Protocol

Primary lymphocytes were cultured in RPMI 1640 media solution (Gibco, Grand Island, NY) with 10% FBS and 2% penicillin streptomycin. These cells were centrifuged at 250 g for 5 minutes at 22°C. If necessary, 5 mL of DPBS was used for washing and the cells were again centrifuged at the previously listed conditions. Then the supernatant was aspirated and the cells were resuspended in new media and passaged or used in an experiment.

2.2 Lymphocyte Separation and Activation

Primary lymphocytes were separated from human whole blood samples. These lymphocytes were activated for lentiviral infections to create CAR T-cells.

2.2.1 Separation Process

Human blood samples were obtained from healthy volunteers at the Clinical Research Center (CRC) in University Park and collected in BD tubes spray-dried with EDTA. Histopaque-1077 (Sigma-Aldrich, St. Louis, MO) and human whole blood samples were brought to room temperature. 3 mL of Histopaque-1077 was added to a 15 mL centrifuge tube and then 3 mL of well-mixed whole blood was layered on top ensuring no mixing occurred between the whole blood and Histopaque-1077 layers. The tubes were then centrifuged at 400 g for 30 minutes at 22°C with a break of 1. After centrifugation, clear layers were present within the tube as shown in the diagram below in **Figure 3**.

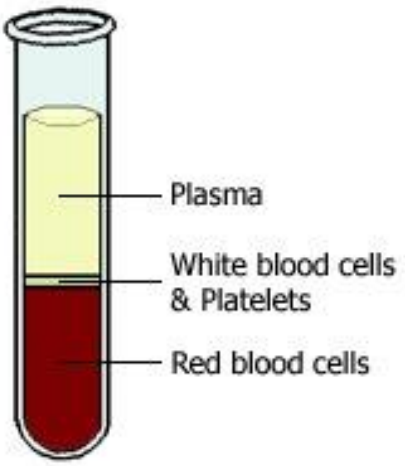

Figure 3: Blood layers present after separation [22]. The middle layer contains the lymphocytes that are of interest.

Excess plasma was aspirated to within 0.5 cm of the buffy coat layer containing white blood cells and platelets. 2 mL of the buffy coat layer was carefully extracted avoiding mixing of layers using a P1000 and added to a new 15 mL centrifuge tube. The cells were washed with 10 mL of DPBS and then centrifuged at 250 g for 10 minutes at 22°C with a break of 5. The supernatant was aspirated and the cells were washed with 5 mL of DPBS and centrifuged again

at the previous conditions. Another washing with 5 mL of DPBS was completed and the cells were resuspended in 1 mL of RPMI media. In a 15 mL centrifuge tube, 10 mL of ACK Lysis Buffer (Gibco, Grand Island, NY) was added and the 1 mL of cells were added on top. This mixture was left at room temperature within a biosafety cabinet for 4 minutes. Then the samples were centrifuged at 300 g for 5 minutes at 22°C and a break of 5. The supernatant was aspirated and the cells were washed with 5 mL of DPBS and centrifuged again at the previous conditions. The supernatant was aspirated and the cells were resuspended in 10 mL of RPMI media to be cultured.

2.2.2 Staining of Lymphocytes

Separated lymphocyte samples were stained with antibodies and analyzed using flow cytometry to determine what percentage of the lymphocytes were T-lymphocytes, the cell of interest. Cells were counted and then diluted to a concentration of $4x10^5$ cells/mL. Four samples of 100 μL of this cell suspension were transferred to an Eppendorf tube. Each tube served as one of four separate experimental groups: a negative control, a secondary control, an IgG control, and the experimental group. All tubes were centrifuged at 2000 RPM for 5 minutes at 4°C. The supernatant was decanted onto a Kimwipe ensuring that the cell pellet was not disturbed. The cell pellet was then resuspended in 500 μL of PBS + 0.1% BSA solution and centrifuged at 2000 RPM for 3 minutes at 5°C. The supernatant was again decanted onto a Kym Wipe, and the cell pellet was resuspended in 100 μL of PBS + 0.1% BSA solution. Then, the primary antibody was added to the necessary tubes. Nothing was added to the negative control and secondary control tubes, 1 μL of mouse IgG1 isotype control antibody (Invitrogen, Carlsbad, CA) was added to the

IgG control tube, and 2 μL of anti-human CD3 antibody (eBioscience, San Diego, CA) was added to the experimental tube. The tubes were then left on ice on a rocker for 2 hours. Following this period, the cells were centrifuged at 1500 RPM for 3 minutes at 4°C and the supernatant was decanted. The cell pellet was then resuspended in 500 μL of PBS + 0.1% BSA solution, after which they were washed three times using the same amount of solution and centrifuge conditions. The cell pellet was then resuspended in 100 μL of PBS + 0.1% BSA solution and 1 μL of the secondary antibody, Alexa Fluor 546 goat anti-mouse (Invitrogen, Carlsbad, CA), was added to all tubes excluding the negative control tube. Then the cells were left on ice for an hour on the rocker. The cells were centrifuged at 1500 RPM for 3 minutes at 4°C and the supernatant was decanted. The cells were resuspended in 500 μL of PBS + 0.1% BSA solution and washed three times. Finally, the cells were resuspended in 300 μL of PBS + 0.1% BSA solution and analyzed using the flow cytometer. FlowJoV10 software was utilized for quantification of the acquired flow cytometer data. The IgG sample was used to draw a gate and the gate was applied to the CD3+ experimental group sample, displaying the percentage of lymphocytes that were T-lymphocytes.

2.2.3 T-Lymphocyte Activation

Dynabeads Human T-Activator CD3/CD28 (Gibco, Grand Island, NY) were used for the activation of T-lymphocytes. First, the Dynabeads were resuspended in the vial using a vortex mixer for 30 seconds. Then the desired volume of Dynabeads was transferred to a 1.5 mL Eppendorf tube. An equal volume of DPBS (or at least 1 mL) was added to the Dynabeads and the mixture was vortexed for 5 seconds. A magnet was placed against the tube for 1 minute and

the supernatant was discarded. The washed Dynabeads were then resuspended in the same volume of RPMI media as the initially extracted volume of Dynabeads. The beads were added at a ratio of 0.5:1 beads to cells to 3 mL of cell suspensions in a 6-well plate. Each well contained $5x10^5$ cells and the cells were incubated for 5 days to allow for proliferation. After five days, the cells were counted and passaged with new Dynabeads to maintain the correct ratio.

2.3 Infection of T-Lymphocytes

Virus containing the TQM-13 CAR plasmid was created by Dr. Lian's lab. Briefly, the TQM-13 CAR DNA was added to a pXL1001 vector (Adgene, Cambridge, MA, USA; plasmid #26122) using restriction enzymes SpeI and EcorRI (Genewiz, South Plainfield, NJ, USA). Then, virus was collected from HEK293 cells. For more in depth information, please reference Appendix A.

Only T-lymphocytes activated using Dynabeads were used in the lentiviral infection. It was assumed that the concentration of virus was approximately 10^6 viruses/mL. For the infection, a ratio of 5 viruses: 1 cell was targeted. The virus was removed from the freezer and kept on ice until use. Activated T-lymphocytes were separated from Dynabeads by transferring the cells and beads to a centrifuge tube and holding a magnet to the cell and bead suspension for 1 minute. Afterwards, the separated cell suspension was transferred to a new centrifuge tube and centrifuged. The supernatant was aspirated and the cells were resuspended in 1 mL of RPMI media. The cells were counted and $1x10^6$ cells were transferred into an Eppendorf tube. The cells were spun down at 2000 RPM for 5 minutes and the supernatant was removed carefully. The cells were resuspended in 100 μL of virus and the correct volume of Dynabeads were added and

the mixture was incubated for 30 minutes. 1.9 mL per well of FBS free RPMI media was added to a 6-well plate. The cell/virus/bead mixture was added to the media and incubated for 16-18 hours. Following the incubation period, the media was changed to RPMI (with FBS) media. After a day, selection was run on the cells using 3 mL of puromysin at a concentration of 1 μg/mL in RPMI (with FBS) media per well.

2.4 Intercellular Gap Opening Experiments

A circular cover glass was added to each well of a 6-well plate. 2 mL of a 70% ethanol/ DPBS solution was added to each well and left for 15 minutes in the biosafety cabinet. The solution was aspirated and 2 mL of DPBS was added to each well for a quick rinse. Then 2 mL of DPBS was added to each well and left for 10 minutes in the biosafety cabinet. After the DPBS was aspirated, 1 mL of a 10 μg/mL fibronectin in BBMVEC media solution was added to the middle of each cover glass and allowed to disperse evenly throughout the well. The lid of the 6-well plate was sealed using Parafilm and left in a 2-8°C refrigerator overnight.

The following day, the fibronectin solution was aspirated and $2x10^5$ BBMVEC cells in 3 mL of media was added to each well. The cells were left to incubate and grow for approximately 5 days when confluent monolayers were present across each cover glass.

If desired, 2 mL of TNF-α at a concentration of 25 ng/mL was added to each well and left to incubate for 6 hours. The media (containing or lacking TNF- α) was aspirated from each well and $6x10^5$ desired cells (lymphocytes or CAR T-cells) in 2 mL of media were added to each well. The 6-well plate was left to incubate for 2 hours. Following the incubation period, the cell solutions were aspirated from each well and 1.5 mL of 4% paraformaldehyde solution was added

to each well. The wells were left for 15 min at room temperature in a biosafety cabinet. Then the 6-well plate was removed from the biosafety cabinet and 2 mL of DPBS was added to each well for 5 minutes. The DPBS was aspirated and a fresh 2 mL of DPBS was added to each well. The 6-well plate was left in the fridge sealed with Parafilm until staining and imaging.

2.4.1 Cell Staining and Imaging

DPBS in each well was aspirated and 1.5 mL of blocking buffer, composed of 0.3% Triton X-100 (Sigma Aldrich, St. Louis, MO) and 5% Goat Serum (Sigma-Aldrich, St. Louis, MO, was added to each well and left on a rocker for 1 hour at room temperature. The blocking buffer was then aspirated and 150 μL of primary antibody solution, VE-Cadherin Rabbit mAb (Cell Signaling Technologies, Danvers, MA), at a concentration of 150 μg/well was added to each cover glass and left to incubate overnight in a 2-8°C refrigerator.

The primary antibody solution was then aspirated and each cover glass was washed 3 times for 5 minutes with 1 mL of DPBS. Then, 150 μL of secondary antibody solution, Alexa Fluor 488 GαR IgG (Life Technologies, Carlsbad, CA), diluted 1:1000, was added to each cover glass and left in the dark at room temperature for at least an hour. The secondary antibody solution was then aspirated and each cover glass was washed for 5 minutes 3 times with 1 mL of DPBS.

Then, 150 μL of Hoechst Stain (Life Technologies, Eugene, OR) was added to each cover glass at a concentration of 2 μg/mL and left in the dark at room temperature for 15 minutes. The stain was aspirated and each cover glass was washed for 5 minutes 3 times with 1 mL of DPBS.

Each cover glass was mounted on a microscope slide using 80 μL of Fluoromount G (SouthernBiotech, Birmingham, AL). Slides were left to dry for around 2 days and imaged using a bright field microscope. A few images were taken at 10x magnification and then 24 images were taken of each cover glass at 100x magnification for analysis.

2.4.2 Gap Opening Analysis

The area of intercellular gap openings between endothelial cells for each of the 24 images taken at 100x magnification was analyzed using ImageJ and divided by the total area of the image to obtain the percentage of gap opening. The average gap opening percentage for each cover glass was calculated. Three cover glass replicates were completed for each experimental group.

2.5 Flow Extravasation Experiments

An endothelial monolayer of BBMVEC cells was grown on Neuro Probe 8 μm pore polycarbonate membrane filters. The filters were placed glossy side up in a Petri dish with 3 mL of 90% ethanol and left under a UV light for 5-10 minutes. This ethanol solution was aspirated and the filter was flipped. A blocker, pictured below in **Figure 4 A)**, was centered on the filter and 1 mL of BBMVEC media without FBS was placed in the center hole. 30 μL of fibronectin was then placed in the media and the dish was left in the incubator overnight. Afterwards, the fibronectin solution was aspirated and silicon strips were placed on either side of the blocker, as shown in **Figure 4 C)**, to prevent movement. 250,000 BBMVEC cells and 1.5 mL of BBMVEC media (with FBS) was added to the center hole. Then 7.5 mL of BBMVEC media (with FBS)

was added to each side of the blocker. The Petri dish was left to incubate for 6 days to allow for the growth of a confluent monolayer. All silicon strips and blockers were autoclaved before use.

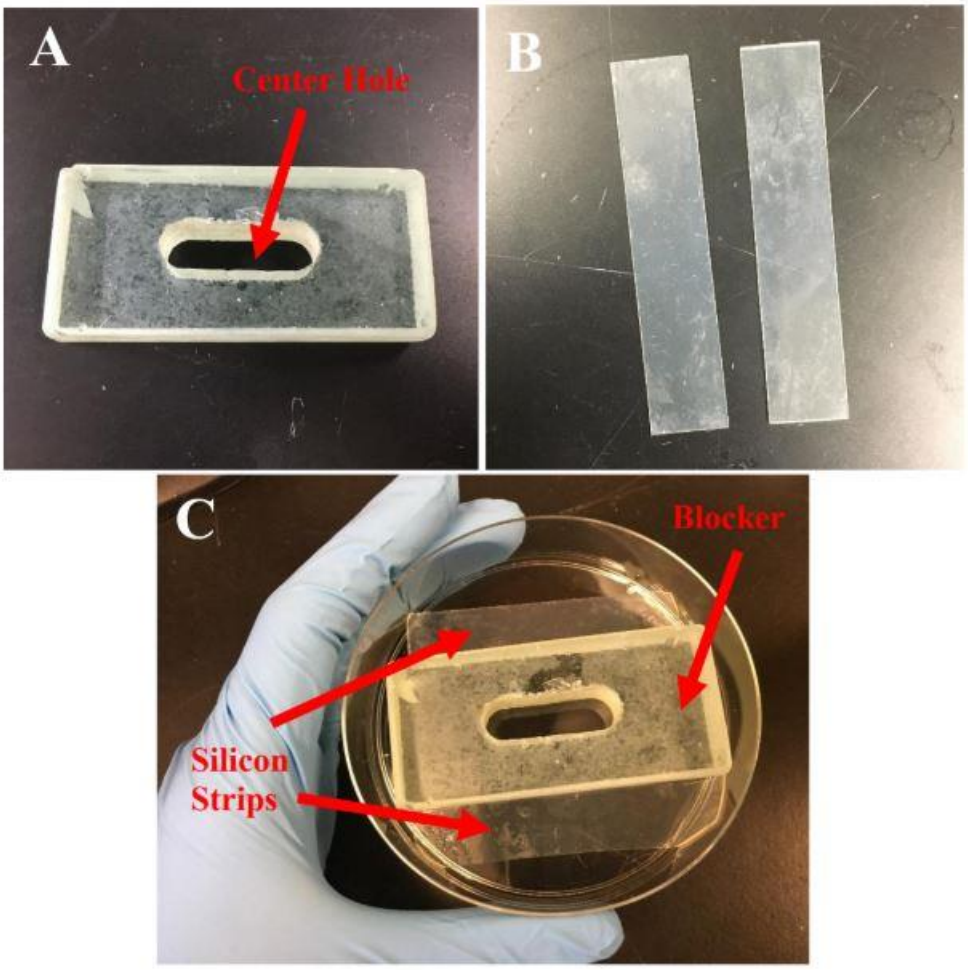

Figure 4: Materials used during the growth of the endothelial monolayer for flow extravasation experiments [23]. A) Blocker used to contain monolayer growth within the center hole. B) Silicon strips used to prevent movement of blocker. C) Full set up used during growth of the monolayer.

The confluent monolayer grown atop the filter was placed within the flow chamber. Flow chamber parts were first washed with soap and hot water and rinsed with DI water. Subsequently, the parts were disinfected in boiling DI water. The bottom plates were submerged for 30 seconds, the top plates were submerged for 20 seconds, and the silicon gaskets were

submerged for 10 seconds. The parts were left to dry before use. Flow chamber parts can be found pictured below in **Figure 5**.

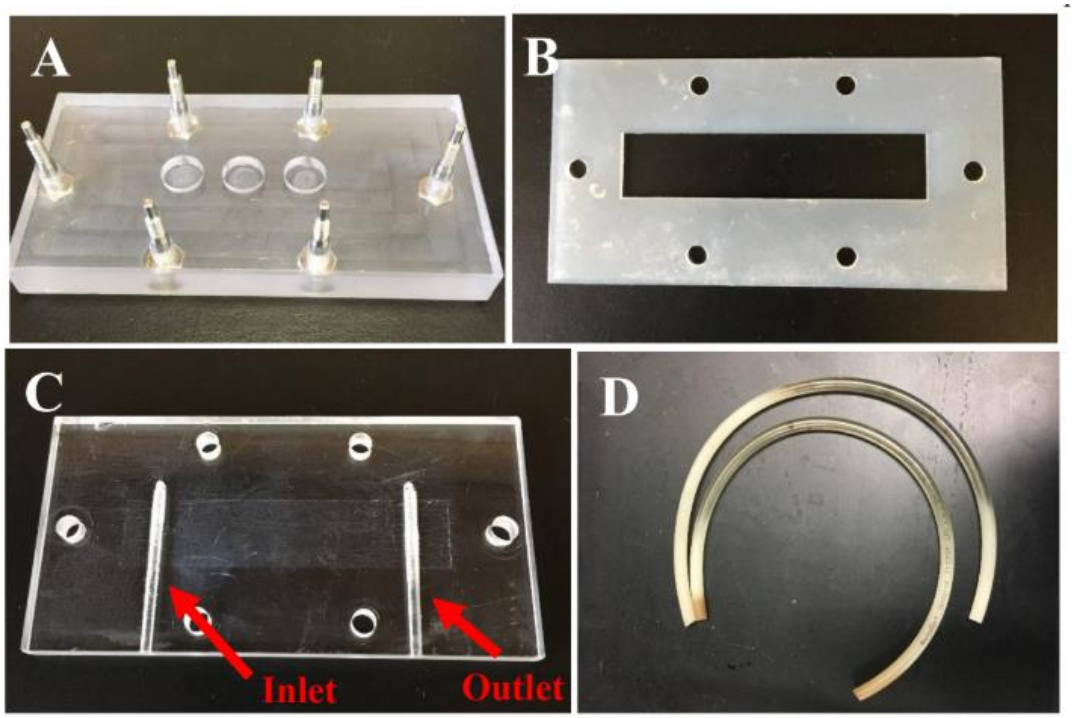

Figure 5: Parts composing the flow chamber [23]. A) Bottom chamber plate with three wells that hold media and chemoattractant. The filter with confluent monolayer was placed atop this bottom chamber plate. B) Silicon gasket that was placed atop the filter containing the confluent monolayer keeping it in place and allowing for the flow of media across the monolayer. C) The top chamber plate including the inlet and outlet that was placed atop the silicon gasket. D) Tubing that was used to connect the assembled flow chamber to the flow chamber box.

A concentration of 2x10^5 cells/mL in 21 mL of media was obtained. This volume was split into two 10 mL volumes that was used as either the inlet or the outlet reservoir. The remaining 1 mL was used as a control for the flow cytometry analysis. A 500 ng/mL solution of C-X-C Motif Chemokine 12 (CXCL12) in RPMI media was created and 200 µL of this solution was placed in each of the wells in the flow chamber's bottom plate.

The filter with the confluent monolayer was placed atop the bottom plate in a manner such that the monolayer covered the length of the three wells. Then, the silicon gasket was

placed atop the filter followed by the top plate and the flow chamber was screwed together. This process is illustrated below in **Figure 6**.

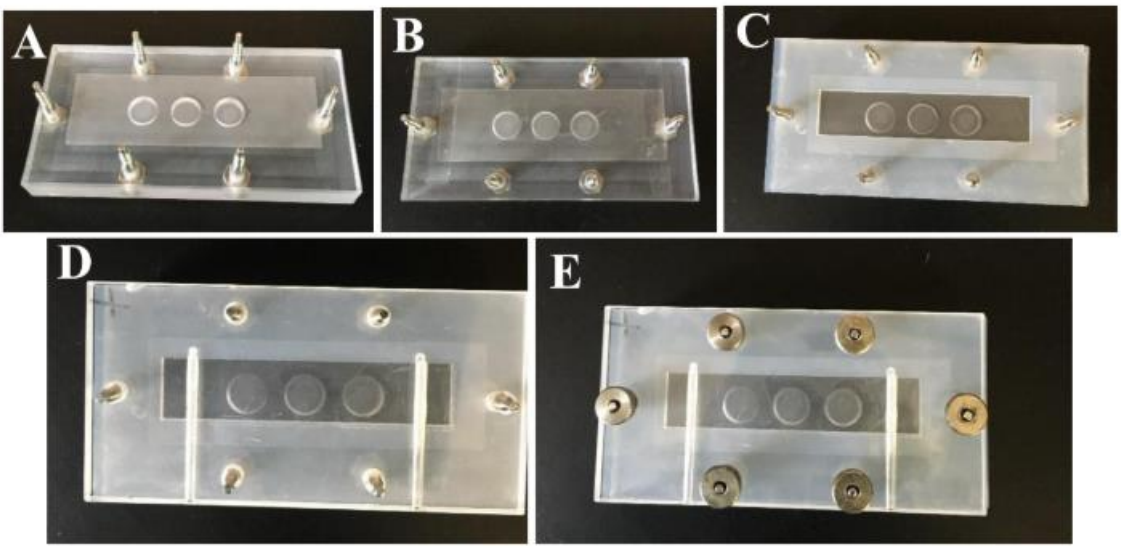

Figure 6: Flow chamber assembly process [23]. A/B) The filter was placed atop the three wells of the bottom plate. C) The silicon gasket was placed on top. D) The top chamber plate is placed on top of the silicon gasket. E) Nuts are attached to the bolts of the bottom chamber to keep the assembled flow chamber together.

Tubes and pipette tips were used to connect the assembled flow chamber to the flow chamber box shown below in **Figure 7**. The flow chamber box was turned on and set to warm to 37°C for at least 45 minutes. Cell solutions were kept in 15 mL centrifuge tubes placed as shown. The motor connected to the flow chamber box was turned on and set to 2 mL/min, which is equivalent to 50 sec^{-1}, and left to run for 4 hours. Then, the motor was stopped and the chambers were removed from the flow chamber box. Solutions in each of the 3 wells of the bottom plates were collected and combined in a 1.5 mL microcentrifuge tube for flow cytometry analysis.

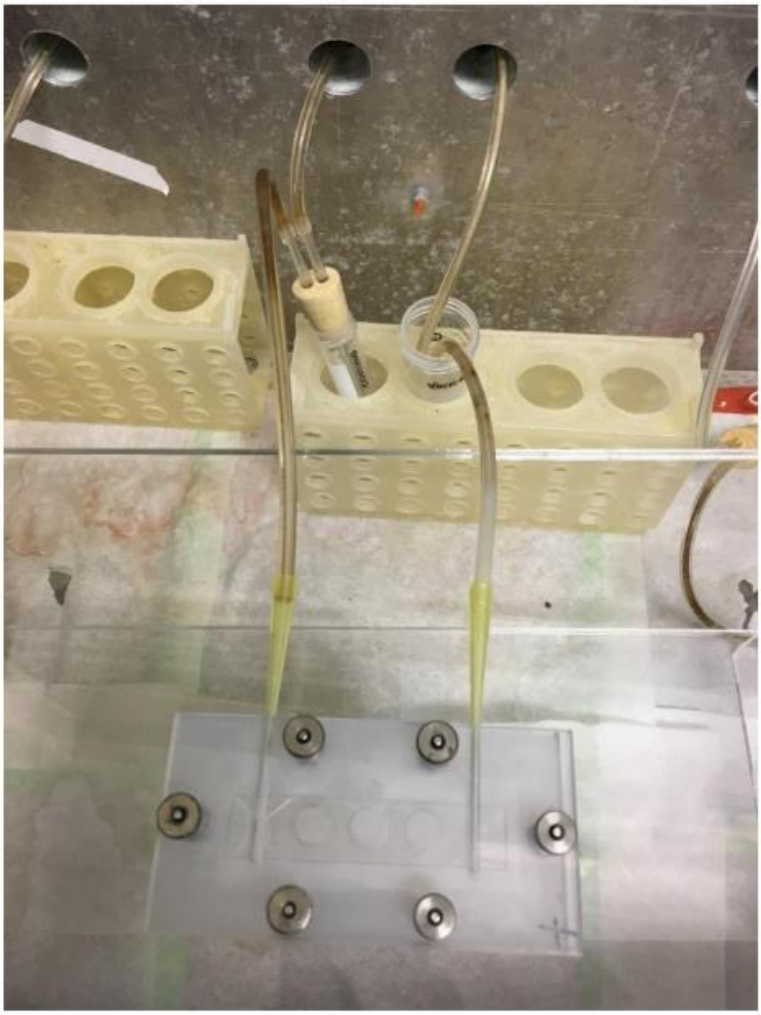

Figure 7: Flow chamber connection to the flow chamber box [23]. Tubing and pipette tips connect the cell suspension reservoirs to the flow chamber leading into the inlet and outlet.

2.5.1 Flow Extravasation Analysis

A Milipore Guava® easyCyte single sample flow cytometer was used to obtain the concentration of migrated cells following the flow migration experiments. The flow cytometer was cleaned using the built-in procedure. Then, data acquisition settings were adjusted utilizing the control sample of cells. Samples from each flow chamber were vortexed and placed in the

flow cytometer. A gate was created for live cells based on the negative control and a concentration of migrated cells in cells/mL was obtained.

2.6 Binding Strength Experiments

U87-LUC cells were grown in 35mmx10mm Petri dishes for the binding strength experiments in the parallel plate flow chamber (Glycotech, Gaithersburg, MD). 500,000 cells in 3 mL of media was left to incubate for 3 days until the monolayer was confluent.

The parallel plate flow chamber gasket (Glycotech, Gaithersburg, MD) was attached smoothly to the parallel plate flow chamber. Then tubing was connected to the inlet, outlet, and vacuum. The inlet tubing leads to the centrifuge tube containing the cell suspension of circulating cells. The outlet tubing leads to the syringe placed in a syringe pump (Harvard Apparatus, Holliston, MA, model #: PHD2000). A diagram illustrating the full set up of the parallel plate flow chamber is included below in **Figure 8**.

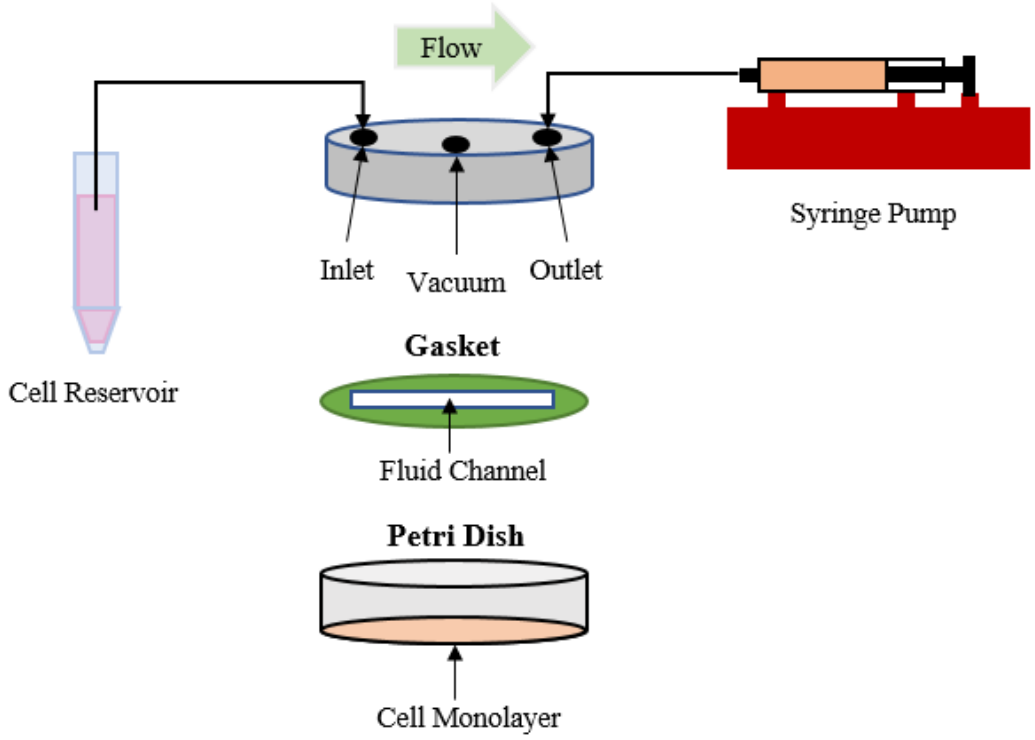

Figure 8: Parallel plate chamber flow loop set up. The parallel plate flow chamber is composed of three parts: a plastic flow deck including an inlet, outlet, and vacuum connection; a gasket containing the fluid channel; and a confluent cell monolayer grown in a Petri dish. A cell reservoir feeds into the inlet of the parallel plate flow chamber. The cell solution then flows across the fluid channel and out through the outlet of the flow chamber into a syringe placed in a syringe pump. The syringe pump is set to provide a constant shear rate throughout the experiment and cell adhesions are observed using a microscope.

Desired cells (lymphocytes or CAR T-cells) were diluted to a concentration of $1x10^6$ cells/mL for circulation. The circulating cells were allowed to settle through slow circulation at 10 s^{-1} for 3 minutes. Then, the syringe pump was set to 50 s^{-1}, 100 s^{-1}, and 200 s^{-1} and flow was recorded for 3 minutes at each setting. According to the geometries of the parallel plate flow chamber, the set shear rates are equivalent to flow rates of 0.02016 mL/min, 0.04032 mL/min, and 0.08064 mL/min respectively.

2.6.1 Binding Strength Analysis

Videos were reviewed and any adhesions between the circulating cells and the U87-LUC cells were characterized as short, intermediate, or long adhesions. Short adhesions lasted less than 30 seconds, intermediate term adhesions lasted between 30-120 seconds, and long adhesions lasted for longer than 120 seconds.

2.7 Statistical Analysis

Two-tailed two-sample t-tests were used to compare lymphocytes and CAR T-cells for all experiments. Results were considered to be statistically significant if the t-test yielded a p-value that was less than 0.05.

Chapter 3

Lymphocyte Separation and Infection

3.1 Motivation

Previous work in this lab has focused on using Jurkat cells, an immortalized line of human T-lymphocyte cells derived from a patient suffering from leukemia. The derivation from a cancer patient and the lack of expression of certain T-lymphocyte receptors on derivative Jurkat cell lines have led to speculation about whether or not they are an adequate model for how primary T-lymphocyte cells truly act *in vivo* [24]. Because of this, a method for T-lymphocyte separation from whole human blood samples was developed. Furthermore, a successful infection protocol with the TQM-13 virus for these separated T-lymphocytes was developed in order to produce viable CAR T-cells for experimentation. The use of these native cells in experiments will allow for results that would better predict what would occur *in vivo* and will allow for direct comparison between the abilities of lymphocytes and CAR T-cells.

3.2 Results

The separation process from whole blood only separated lymphocytes from other blood components and did not specifically target T-lymphocytes. Due to this, the percentage of T-lymphocytes present in the separated lymphocytes was quantified. Following the solidification of

a separation protocol, successful infection of the T-lymphocytes with the CAR vector was confirmed.

3.2.1 T-Lymphocyte Separation Quantification

After the lymphocyte separation process, an anti-CD3 antibody was utilized to target only the T-lymphocytes present in the separated lymphocytes. Whole blood was separated three separate times and this quantification process was run on each replicate. The flow cytometry results are displayed below in **Figure 9**. This data concluded that on average, 75.2% +/- 2.3% (SEM) of the separated lymphocytes are T-lymphocytes.

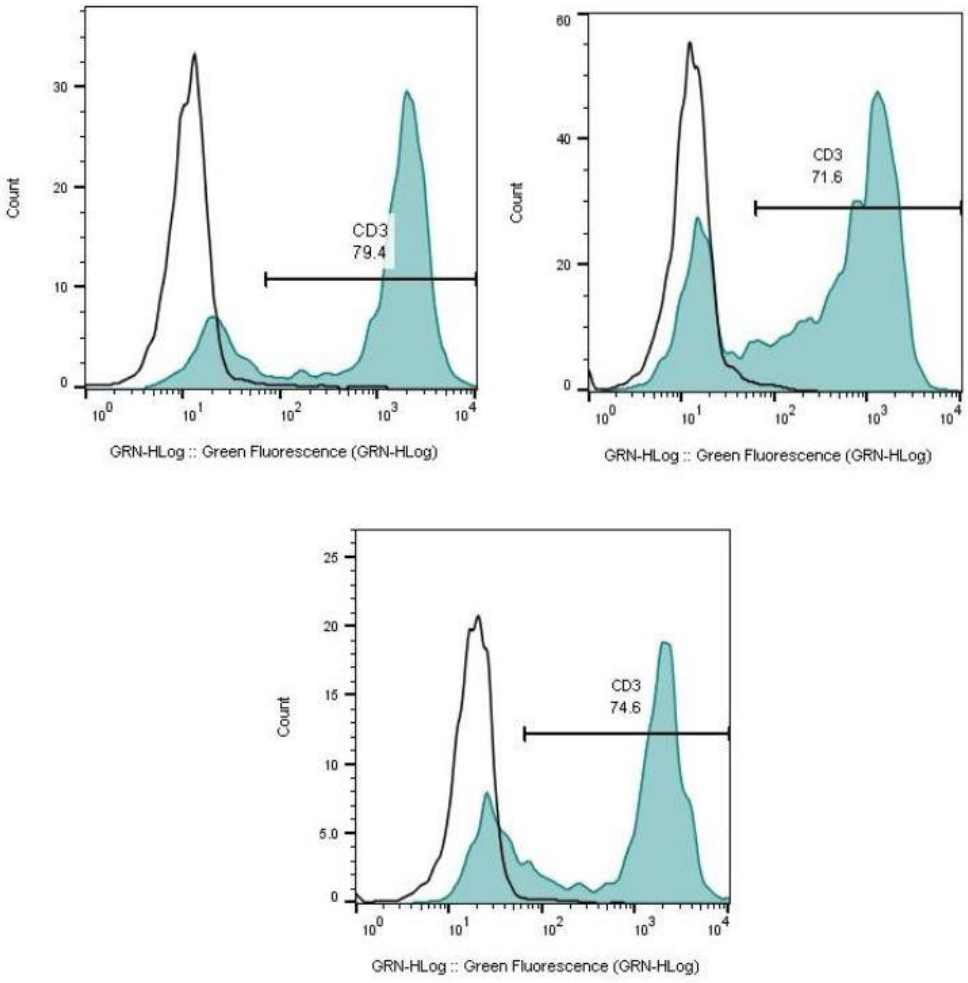

Figure 9: Flow cytometry results quantifying the percentage of T-lymphocytes separated. Three replicates of the T-lymphocyte quantification process were run resulting in an average of 75.2% +/- 2.3% (SEM) of T-lymphocytes present in the separated lymphocytes. Sections colored in blue were cells stained with the anti-CD3 antibody. Sections with a black outline were cells stained with an IgG control antibody.

3.2.2 Infection of Lymphocytes

After confirming that a large majority of T-lymphocytes were present in the separated lymphocytes, infections with the TQM-13 CAR vector were conducted and verified to have been successful. Unfortunately, the CAR vector was not fluorescent in nature and therefore impossible to track to ensure that the infection had been carried out successfully. To solve this problem,

another vector displaying a GFP construct was created and separate samples of T-lymphocytes were simultaneously infected with the GFP CAR vector and the TQM-13 CAR vector. As the T-lymphocytes used were from the same separation sample and the same infection procedure and timeline were used, it can be assumed that if the T-lymphocytes infected with the GFP vector displayed fluorescence (indicating a successful infection), then the T-lymphocytes infected with the TQM-13 vector were also successfully infected. In addition, it was confirmed that T-lymphocytes infected with the TQM-13 vector looked as healthy as those infected with the GFP vector. **Figure 10** displays the results 24 hours after a successful infection of T-lymphocytes with the GFP CAR vector.

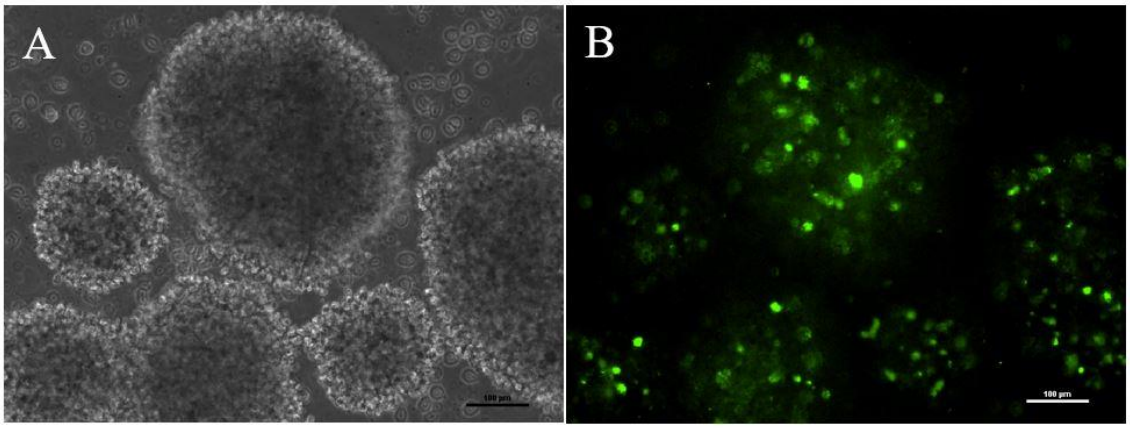

Figure 10: Successful GFP CAR vector infection results. Scale bars represent 100 µm. A) Bright field microscope picture displaying infected T-lymphocytes. The cell clumping indicates healthy and viable cells. Dark black spots seen are Dynabeads used for T-lymphocyte activation. B) Fluorescent microscope picture of the same T-lymphocytes. Successfully infected cells with the GFP CAR vector display green fluorescence.

3.3 Discussion

These experiments provided confirmation that further experimentation on T-lymphocytes, both infected and not infected with TQM-13 CAR vectors could be performed. The quantification of T-lymphocytes separated showed that a large majority of the separated

lymphocytes were in fact T-lymphocytes. Additionally, the infection process using the GFP vector showed a large percentage of the T-lymphocytes fluorescing, indicating a successful infection. T-lymphocytes that were infected with the TQM-13 vector at the same time as the pictured GFP vectors looked equally as healthy. Therefore, it can be assumed that the infection with the TQM-13 CAR vector was also successful. These infection results were used as a benchmark for future infections to confirm success.

Chapter 4

Static Intercellular Gap Opening Studies

4.1 Background and Motivation

Many considerations must be made when determining whether CAR modified T-lymphocytes would be able to effectively target GBM. One important consideration is the ability of the CAR T-cells to open tight junctions intercellularly within the BBB, which allows for subsequent extravasation of lymphocytes through the endothelial layer. The migration of lymphocytes and other immune cells through an endothelial layer is composed of four steps, illustrated below in **Figure 11.** The first step involves the interaction between the lymphocyte and the endothelial cell receptors, which leads to the slowing of cell rolling. Then, interactions between the lymphocytes with chemokines found on the surface of the endothelial cells leads to activation of integrins and consequently the firm adhesions of lymphocytes to the endothelial cell. The fourth and final step involves the diapedesis of the lymphocyte which occurs either through the endothelial cell or between the endothelial cells [25].

Specific to lymphocytes, cell rolling begins with the short interactions between selectins found on the endothelial layer with glycosylated ligands expressed by T-lymphocytes, such as P-selectin glycoprotein ligand-1 and CD44. Lymphocytes display catch bond adhesions. This means that when they are subjected to shear rates below a threshold, they flow freely. However, once above the shear threshold, interactions between the lymphocytes and endothelial receptors begin during cell rolling. During rolling, lymphocytes pause while the lymphocyte and endothelial receptor bonds are intact. These bonds eventually break and the lymphocytes roll forward until another bond forms. This rolling reduces the cell velocity and allows for T-

lymphocytes to eventually interact with integrin ligands, which have slower kinetics, on the endothelial layer that were activated by chemokines. Once bound to the receptors, an increase in shear rate reinforces the binding, resulting in the complete stop of the lymphocytes during firm adhesions [26]. Two of the main integrins found on lymphocytes are the β2 integrin, lymphocyte function-associated antigen 1 (LFA-1), composed of CD11a/CD18 and the α4β1 integrin, very late antigen-4 (VLA-4), composed of CD49d/CD29. LFA-1 binds to intercellular adhesion molecule type-1 and 2 (ICAM-1 and ICAM-2) expressed by the endothelial layer while VLA-4 binds to vascular cell adhesion molecule type 1 (VCAM-1). Transendothelial migration follows the firm adhesion of the integrins to their corresponding ligands [28].

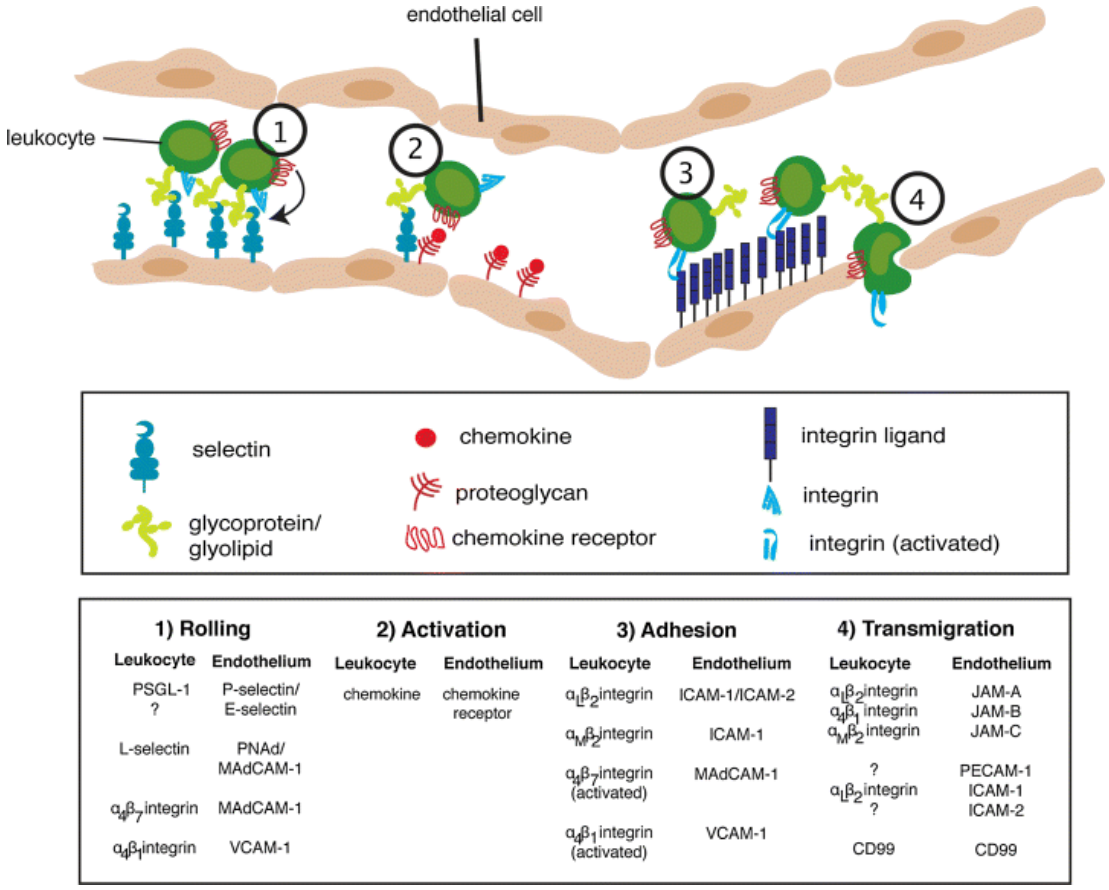

Figure 11: Adhesion cascade that leads to the migration of leukocytes across an endothelial wall [28].

During intercellular diapedesis of lymphocytes between endothelial cells, tight junctions between the endothelial cells must be opened. The number of tight junctions that are opened intercellularly will be quantified using static gap studies and a comparison of lymphocytes and CAR T-cells will be performed. This information will provide valuable knowledge on whether the CAR modification process affects the ability of lymphocytes to open tight junctions within the BBB, therefore modifying their ability to migrate across the BBB and reach the target tumor site. This chapter's work focuses on intercellular diapedesis of lymphocytes while the work completed in Chapter 5 will encapsulate both types of diapedesis.

4.1.1 Use of Tumor Necrosis Factor (TNF-α)

TNF-α is a pro-inflammatory cytokine that is mainly secreted by macrophages and differentiated helper T-lymphocytes [27] and is known to affect vascular endothelium [30]. Specifically, TNF-α increases the permeability of the endothelium and upregulates cell adhesion molecules including E-selectin, ICAM-1, and VCAM-1. As mentioned previously, T-lymphocytes express LFA-1, which binds to the ICAM-1 receptor, and VLA-4, which binds to VCAM-1, so it is hypothesized that treatment of the BBMVEC endothelial monolayer with TNF-α will enhance the adhesion cascade, and increase the number of tight junctions opened. A maximum expression level of ICAM-1 was seen after 6-8 hours of treatment with TNF-α [27]. Using this information, BBMVEC endothelial monolayers were treated with TNF-α for 6 hours prior to experimentation for the static gap studies discussed here.

4.2 Results

A full factorial experimental design was utilized for the static intercellular gap experiments. Overall gap formation was measured for control, unmodified T cells, or CAR T-cells with or without the presence of TNF-α. Following an incubation time of 2 hours (after a 6-hour incubation with TNF-α, if applicable) cells were fixed and imaged. Gap formation as a percentage of total monolayer area was determined for each experimental group. The results are displayed below in **Figure 12**.

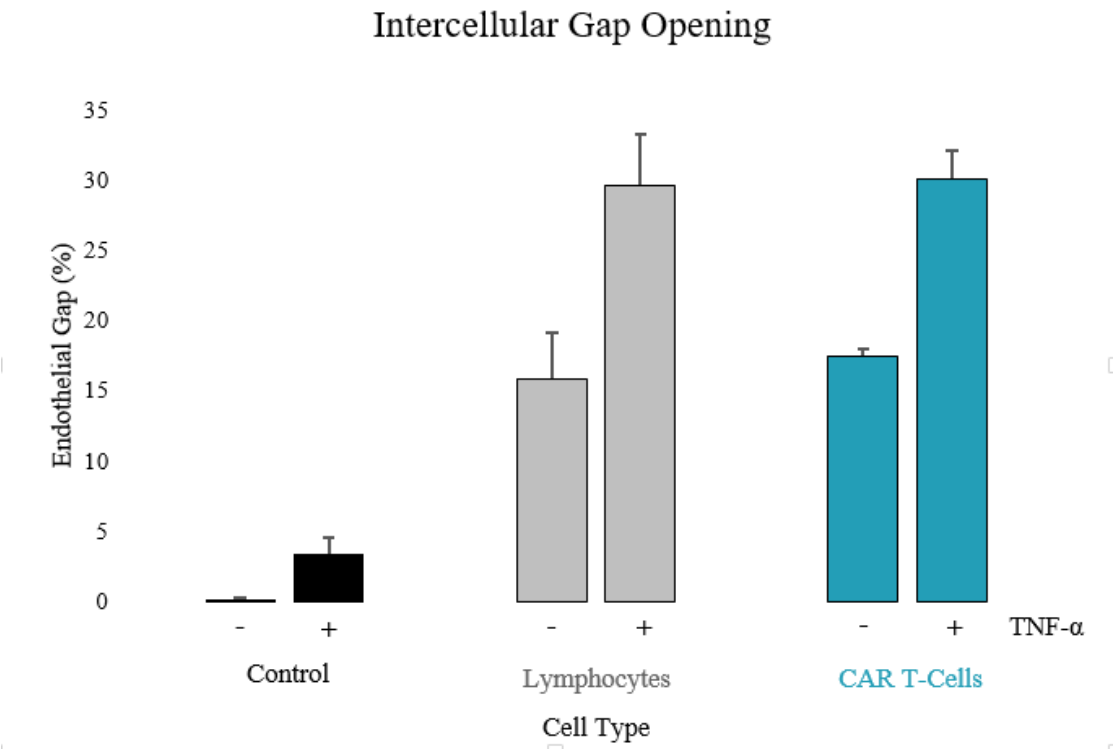

Figure 12: Static intercellular gap study results. Analyzed results showing the percentage of gap openings observed for each cell type with and without TNF-α pretreatment. Results represent the mean +/- SEM with an n=3 (*p<0.05).

The ability of unmodified lymphocytes and CAR T-cells to form gaps in the endothelial monolayer was not found to be significantly different. However, pretreatment with TNF- α resulted in a significant increase in gap formation for both lymphocyte and CAR T-cell groups.

4.3 Discussion

From the averages obtained for the three replicates run for each experimental group, it was observed that CAR T-cells may open a slightly higher percentage of gaps than unmodified lymphocytes. However, the difference in gap formation between the lymphocytes and CAR T-cells was determined to be insignificant. This indicates that CAR modification of the lymphocytes did not impair the cells' innate ability to open tight junctions within the endothelial monolayer. This information implies that CAR T-cells can open up the BBB at least as well as unmodified lymphocytes *in vivo*, reinforcing the idea that it is a viable treatment for GBM.

When looking at the p-values comparing significance of TNF-α pretreatment in opening intercellular gaps, for both the lymphocyte and CAR T-cell groups, the TNF-α did make a statistically significant difference. This suggests that when combined with a treatment of lymphocytes or CAR T-cells, TNF-α increases the amount of intercellular gaps opened. This finding agrees with information found in literature indicating that the pretreatment of TNF-α does increase the ability of cells to open tight junctions within an endothelial layer.

Chapter 5

Flow Extravasation Studies

5.1 Background and Motivation

In order for cells to effectively cross the BBB, they must be able to successfully extravasate, the final step of the adhesion cascade mentioned previously in Chapter 4. The protocol for the flow extravasation chamber using BBMVEC cells has been tested and confirmed in previous work completed by Nmachi Anumba [23].

C-X-C motif chemokine 12 (CXCL12), also known as stromal cell-derived factor 1 (SDF1), is a chemokine protein that has been proven to be a strong chemoattractant attracting and stimulating transendothelial chemotaxis in lymphocytes [31]. Additionally, CXCL12 and its receptor CXCR4, are expressed in increasing levels corresponding to increasing levels of tumor grade in many malignant tumors, including gliomas [32]. Due to these characteristics, CXCL12 was selected to be the chemoattractant added to wells in the flow chamber's bottom plate.

This chapter's work focuses on the comparison of the ability of T-lymphocytes and CAR T-cells to extravasate through a mock BBB consisting of BBMVEC cells. This comparison provides further important insight into the potential impact that the CAR modification may have on the ability of lymphocytes to migrate across the BBB.

5.2 Results

A filter, bearing a monolayer of BBMVEC cells, was assembled within the flow chamber. Lymphocytes and CAR T-cells were circulated through the flow loop and flow chamber for four hours. Afterwards, samples were collected from the wells of the bottom chamber plate and cell concentrations were obtained using flow cytometry. The results are displayed below in **Figure 13**. Statistical analysis comparing the concentration of migrated cells between lymphocytes and CAR T-cells did not find a significant difference.

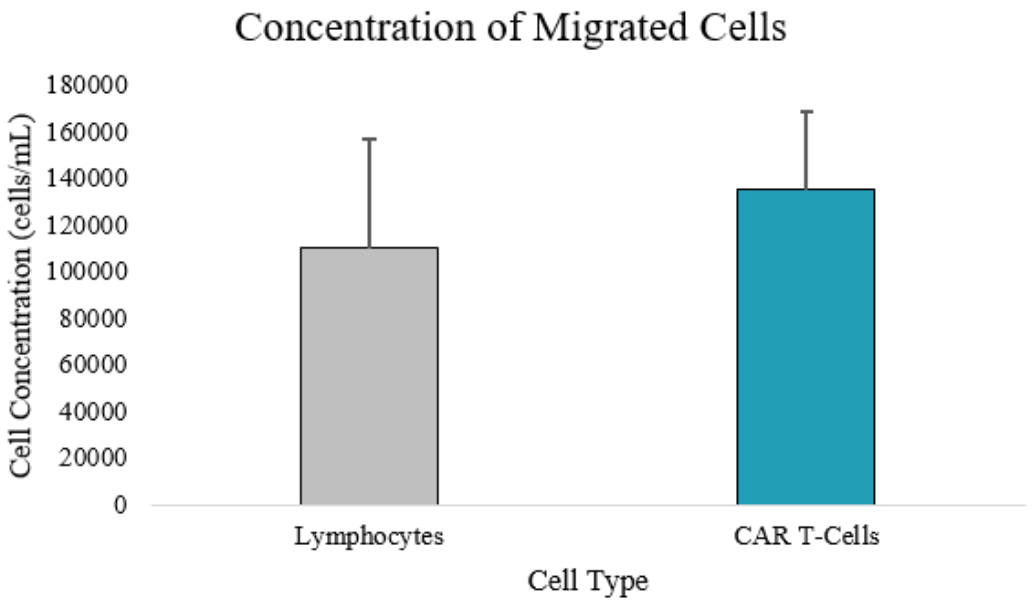

Figure 13: Concentration of cells that successfully migrated through the *in vitro* model of the BBB. Cell concentrations were collected using flow cytometry. Results represent the mean +/- SEM with an n=3.

5.3 Discussion

T-test analysis determined that the difference in transendothelial cell migration between groups was statistically insignificant. Consistent with those observed in Chapter 4, these results imply that CAR modification of the lymphocytes does not impair the ability of the cells to

migrate through the mimic BBB. This further supports its use as a glioblastoma cancer immunotherapy.

Chapter 6

Binding Assay Studies

6.1 Motivation

Arguably, the most important aspect of CAR T therapy is selecting the appropriate tumor antigen to target. An appropriately selected CAR receptor targeting GBM should result in CAR T-cells that display stronger binding to GBM cells. Correct and selective binding to the target tumor cells is the first step in the activation of the CAR T-cell therapy. This chapter's work focuses on exploring the binding strength between TQM-13 CAR T-cells or unmodified lymphocytes to GBM cells to assess the validity of the TQM-13 CAR design.

6.2 Results

A parallel plate flow chamber was utilized to perform binding assays. Lymphocytes and CAR T-cells were flowed atop a monolayer of U87-LUC GBM cells for three minutes at three different shear rates of 50, 100, and 200 s^{-1}. Any observed adhesions were characterized as short, intermediate, or long. Short adhesions lasted for less than or equal to 30 seconds, intermediate adhesions lasted between 30 to 120 seconds, and long adhesions lasted for longer than or equal to 120 seconds. The resulting quantified adhesions at each shear rate are displayed below in **Figure 14**.

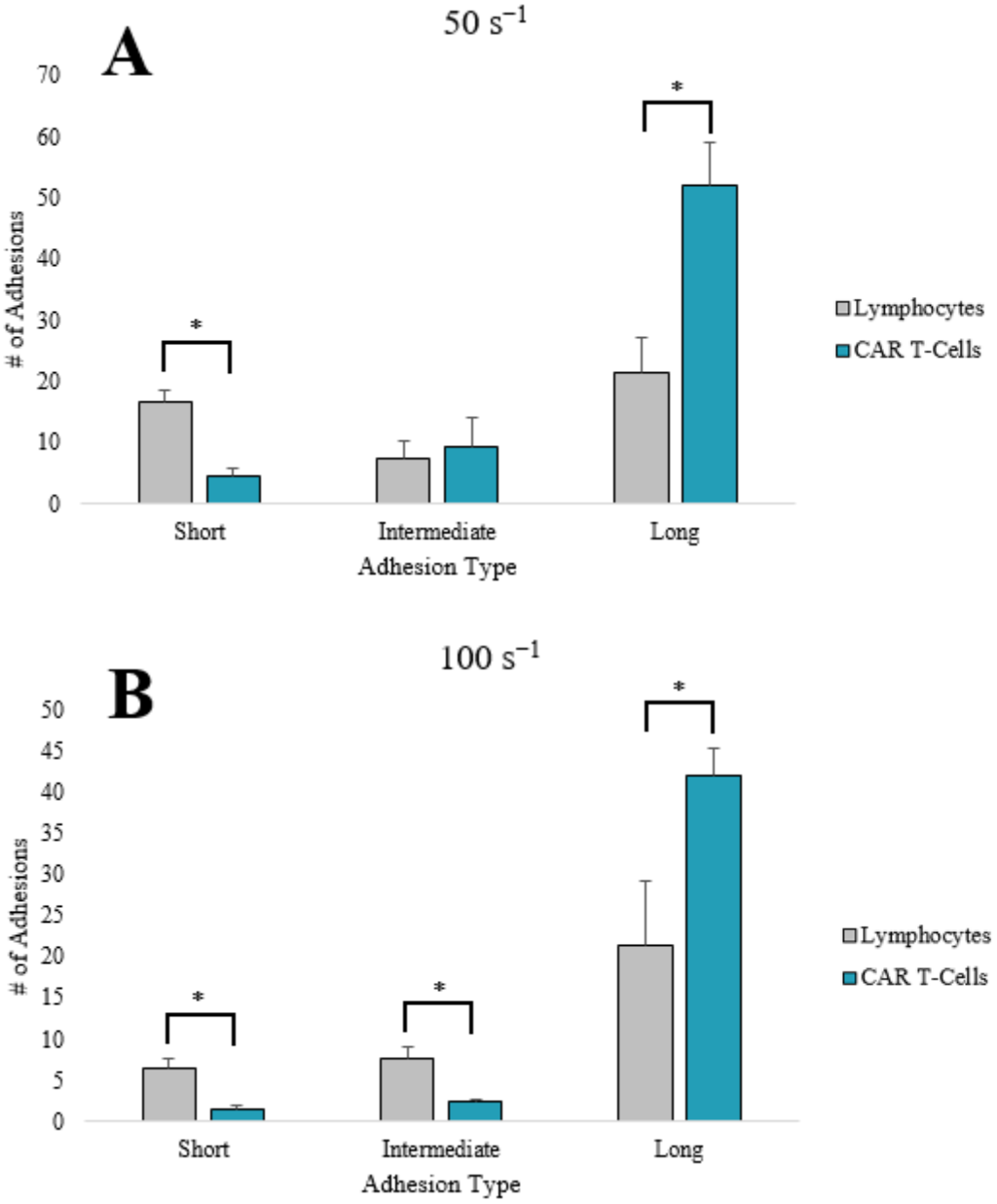
A
50 s−1
70
60
50
40
30
20
10
0
# of Adhesions
*
*
Short
Intermediate
Long
Adhesion Type
Lymphocytes
CAR T-Cells
B
100 s−1
50
45
40
35
30
25
20
15
10
5
0
# of Adhesions
*
*
*
Short
Intermediate
Long
Adhesion Type
Lymphocytes
CAR T-Cells

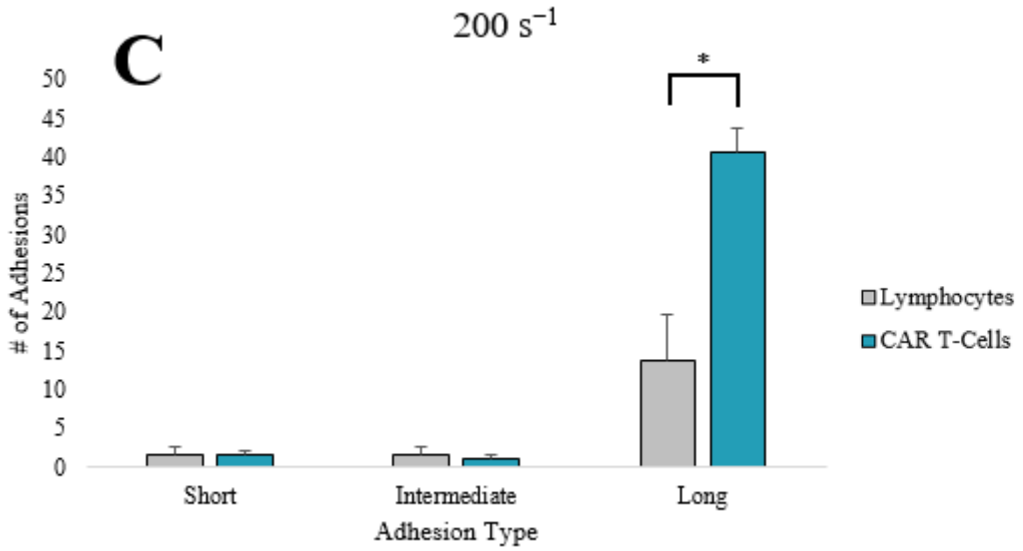

Figure 14: Adhesions observed between lymphocytes and CAR T-cells and GBM cells at three different shear rates. Adhesions were quantified by binding time as short, intermediate, or long. A) shows the adhesions observed at 50 s^{-1}, B) shows the adhesions observed at 100 s^{-1}, and C) shows the adhesions observed at 200 s^{-1}. Results represent the mean +/- SEM with an n=3 (*$p<0.05$).

6.3 Discussion

Lymphocytes displayed significantly more short adhesions at shear rates of 50 s^{-1} and 100 s^{-1}, and more intermediate adhesions at 100 s^{-1}. However, the amount of long adhesions are the adhesions of importance. When analyzing the ability of the CAR T-cells to effectively target the GBM cells, longer adhesions display more prolonged and stronger attachments, which translates to stronger binding and attachment. At each shear rate, CAR T-cells displayed significantly more long adhesions than lymphocytes. Additionally, CAR T-cells consistently resulted in more total adhesions than lymphocytes, with the majority of these adhesions being classified as long. These trends further support the fact that the lymphocytes were successfully infected with the TQM-13 CAR virus. More importantly, it provides promising data supporting the claim that TQM-13 CAR T-cells can effectively target and bind to GBM cells.

Chapter 7

Conclusion

7.1 Summary of Findings

Two of the major obstacles encountered in utilizing CAR T immunotherapy in the treatment of GBM are ensuring passage through the BBB and selection of an appropriate and effective target antigen. The work completed throughout this paper addressed each of these obstacles, analyzing the extravasation abilities of CAR modified T-lymphocytes and the ability of CAR T-cells expressing TQM-13 to effectively target GBM cells.

Using static intercellular gap opening assays, it was found that the TQM-13 CAR modification led to a statistically insignificant change in intercellular gap opening. Additionally, a flow extravasation chamber showed that the TQM-13 CAR T-cells also displayed a statistically insignificant change in transendothelial extravasation abilities. These results show that the CAR modification does not impede the innate ability of T-lymphocytes to open intercellular gaps between and migrate through the BBB. Additionally, binding strength assays utilizing a parallel plate chamber showed that the CAR T-cells demonstrated significantly more long adhesions at three different shear rates, as well as more total adhesions. These findings validate the TQM-13 CAR design, as the CAR T-cells displayed significantly stronger binding and prolonged interaction with the target GBM cells.

Overall, the results attest to the potential of CAR T-cells expressing TQM-13 as a successful immunotherapy for treatment of GBM. These CAR T-cells are able to overcome the BBB, a challenge faced by many other GBM treatments, and also show enhanced affinity toward GBM cells.

7.2 Future Work

The results obtained from this study set the groundwork for future work expanding upon single receptor CAR modifications of T-lymphocytes. Work has already been completed within the lab regarding the addition of biodegradable photobleaching-resistant fluorescent polymer polylactide copolymer (BPLP-PLAs) nanoparticles containing doxorubicin to CAR T-cells. This addition expands upon the efficacy of CAR T-cells, as the CAR modification serves as a transport mechanism to bring the nanoparticles to the tumor site where they will then aid the CAR T-cells in eradication of the tumor. Specifically, the toxicity of free-flowing nanoparticles containing doxorubicin and drug-containing nanoparticles clicked to CAR T-cells to GBM cells will be compared. This innovative combination of technologies can be applied to different cancer types. Additionally, further work involving CAR T-cells targeting multiple receptors is of interest. A second CAR design targeting a receptor expressed uniquely by brain endothelial cells will be added in addition to the TQM-13 CAR receptor in order to increase the amount of CAR T-cells that reach the BBB, thereby increasing the efficiency of the therapy process.

Appendix A: TQM-13 CAR Virus Production Protocol [33]

Construction of pXL001- IL13CAR

The IL13 CAR gene was synthesized and cloned into the pXL001 vector upon removal of tTR-KRAB using restriction enzymes SpeI and EcoRI (Genewiz, South Plainfield, NJ, USA). pXL001 was a gift from Sean Palecek (Addgene, Cambridge, MA, USA; plasmid # 26122).

Generation of lentiviruses

To generate lentiviruses containing the pXL001- IL13CAR plasmid, cargo plasmid (pXL001- IL13CAR) and 2nd generation packaging plasmids psPAX2 and pMD2.G were added into OptiMEM from Invitrogen (Invitrogen, Carlsbad, CA, USA; catalog #: 31985070) and incubated at room temperature for 5 minutes. psPAX2 and pMD2.G were gifts from Didier Trono (Addgene, Cambridge, MA, USA; plasmid # 12260 and 12259). Fugene HD reagent (Promega, Madison, WI, USA; catalog #: E2311) was added mixed by careful pipetting before incubating at room temperature for 10-15 minutes. This solution was then added into pre-warmed DMEM+10% FBS to make the transfection media. Media was changed on 90% confluent HEK293 cells using ½ the normal culture volume of transfection media. Cells were incubated overnight at 37°C and media was changed the following morning with pre-warmed DMEM + 10% FBS using 1 ½ the normal culture volume. 24hrs, 48hrs, and 72hrs after this media change, virus containing media was collected from the cells and the media was changed with pre-warmed DMEM + 10% FBS using 1 ½ the normal culture volume. The cells were disposed of after the third collection. For unconcentrated virus solution, immediately following

collection, the virus containing media was centrifuged for 5 minutes and the supernatant was collected and stored at -80C. For concentrated virus solution, the collected virus containing media is stored at 4C until collection is complete. Virus containing media is centrifuged for 5 minutes and the supernatant is collected. Concentration is done using Lenti-X Concentrator (Takara Bio, Mountain View, CA, USA; catalog #: 631231).

Lentiviral infection of HEK 293 cells

To infect HEK293 cells, 200uL of fresh virus containing media is added directly into the culture media of those cells and pipetted to mix.

BIBLIOGRAPHY

[1] Quick Brain Tumor Facts. (n.d.). Retrieved from http://braintumor.org/brain-tumor-information/brain-tumor-facts/

[2] Treatment Options. (n.d.). Retrieved from http://braintumor.org/brain-tumor-information/treatment-options/

[3] Glioblastoma (GBM) | American Brain Tumor Association | Learn More. (n.d.). Retrieved from https://www.abta.org/tumor_types/glioblastoma-gbm/

[4] Why Cancer Immunotherapy. (n.d.). Retrieved from https://www.parkerici.org/why-cancer-immunotherapy/?cn-reloaded=1

[5] Blood-brain Barrier Permeability. (n.d.). Retrieved from https://www.rndsystems.com/research-area/blood--brain-barrier-permeability

[6] Blood-Brain Barrier | Neuroscience Research. (n.d.). Retrieved from https://www.tocris.com/research-area/blood-brain-barrier

[7] Serlin, Y., Shelef, I., Knyazer, B., & Friedman, A. (2015, February). Anatomy and physiology of the blood–brain barrier. In Seminars in cell & developmental biology (Vol. 38, pp. 2-6). Academic Press.

[8] Research Research Interest | Lab Facilities | Research Grants. (n.d.). Retrieved from http://www.bme.cuhk.edu.hk/jchchoi/r_SHIAE14-16.php

[9] Banks, W. A. (2009, June). Characteristics of compounds that cross the blood-brain barrier. In BMC neurology (Vol. 9, No. 1, p. S3). BioMed Central.

[10] Daneman, R., & Prat, A. (2015). The Blood--Brain Barrier. Cold Spring Harb Perspect Biol.

[11] Larochelle, Catherine, Alvarez, Jorge, and Prat, Alexandre. “How do immune cells overcome the blood-brain barrier in multiple sclerosis?” FEBS Letters 585. 3770-3780. Print.

[12] Wong, A. D., Ye, M., Levy, A. F., Rothstein, J. D., Bergles, D. E., & Searson, P. C. (2013). The blood-brain barrier: an engineering perspective. Frontiers in neuroengineering, 6, 7. doi:10.3389/fneng.2013.00007

[13] Méresse, S., Dehouck, M. P., Delorme, P., Bensaïd, M., Tauber, J. P., Delbart, C., ... & Cecchelli, R. (1989). Bovine brain endothelial cells express tight junctions and monoamine oxidase activity in long-term culture. Journal of neurochemistry, 53(5), 1363-1371.

[14] NCI Dictionary of Cancer Terms. (n.d.). Retrieved from https://www.cancer.gov/publications/dictionaries/cancer-terms/def/car-t-cell-therapy

[15] Dotti, G., Gottschalk, S., Savoldo, B., & Brenner, M. K. (2014). Design and development of therapies using chimeric antigen receptor-expressing T cells. Immunological reviews, 257(1), 107-126.

[16] Weighing the Cost and Value of CAR T-Cell Therapy. (n.d.). Retrieved from http://www.ascopost.com/issues/may-25-2018/weighing-the-cost-and-value-of-car-t-cell-therapy/

[17] DeMarco, C. (n.d.). 9 things to know about CAR T-cell therapy. Retrieved from https://www.mdanderson.org/publications/cancerwise/car-t-cell-therapy--9-things-to-know.h00-159221778.html

[18] Novel T-Cell Therapies Make Inroads Into Solid Tumors. (n.d.). Retrieved from https://www.onclive.com/publications/oncology-live/2018/vol-19-no-22/novel-tcell-therapies-make-inroads-into-solid-tumors

[19] Van Nguyen, J. M. C., Zhu, D., Gibo, D. M., Hantgan, R. R., Larson, S. M., Debinski, W., & Mintz, A. (2012). A novel ligand delivery system to non-invasively visualize and therapeutically exploit the IL13Rα2 tumor-restricted biomarker. Neuro-Oncology, 14(10), 1239.

[20] Thaci, B., Brown, C. E., Binello, E., Werbaneth, K., Sampath, P., & Sengupta, S. (2014). Significance of interleukin-13 receptor alpha 2–targeted glioblastoma therapy. Neuro-oncology, 16(10), 1304-1312.

[21] Brown, C. E., Badie, B., Barish, M. E., Weng, L., Ostberg, J. R., Chang, W., . . . Jensen, M. C. (2015). Bioactivity and Safety of IL13Ra2-Redirected Chimeric Antigen Receptor CD8 T Cells in Patients with Recurrent Glioblastoma. Clinical Cancer Research.

[22] Dean, L. (2005). Blood Groups and Red Cell Antigens [Internet]. Bethesda (MD): National Center for Biotechnology Information (US). Blood and the cells it contains.

[23] Anumba, N. (2018). Development of Feasibilities for Immune Cell-Mediated Nanoparticle Transport Through the Endothelial Barrier Under Flow Conditions.

[24] Abraham, R. T., & Weiss, A. (2004). Jurkat T cells and development of the T-cell receptor signalling paradigm. Nature Reviews Immunology, 4(4), 301.

[25] How do immune cells overcome the blood–brain barrier in multiple sclerosis? (2011, May 04). Retrieved from https://www.sciencedirect.com/science/article/pii/S001457931100336X

[26] Thomas, W. (n.d.). Catch Bonds in Adhesion. Annual Review of Biomedical Engineering 2008, 39-57.

[27] TNF tumor necrosis factor [Homo sapiens (human)] - Gene - NCBI. (n.d.). Retrieved from https://www.ncbi.nlm.nih.gov/gene/7124

[28] Mitroulis, I., Alexaki, V. I., Kourtzelis, I., Ziogas, A., Hajishengallis, G., & Chavakis, T. (2015). Leukocyte integrins: role in leukocyte recruitment and as therapeutic targets in inflammatory disease. Pharmacology & therapeutics, 147, 123-135.

[29] Weninger, W. (2006, September 14). Immune cell migration as a means to control immune privilege: Lessons from the CNS and tumors. Retrieved from https://onlinelibrary.wiley.com/doi/full/10.1111/j.1600-065X.2006.00433.x

[30] Carman, C., Sage, P., Sciuto, T., De la Fuente, M., Geha, R., Ochs, H., . . . Springer, T. (n.d.). Transcellular Diapedesis is Initiated by Invasive Podosomes.

[31] Bleul, C. C., Fuhlbrigge, R. C., Casasnovas, J. M., Aiuti, A., & Springer, T. A. (1996). A highly efficacious lymphocyte chemoattractant, stromal cell-derived factor 1 (SDF-1). Journal of Experimental Medicine, 184(3), 1101-1109.

[32] Miyazaki, T., Uemae, Y., & Ishikawa, E. (2017). CXCL12/CXCR4 signaling in glioma stem cells—prospects for therapeutic intervention. Translational Cancer Research, 6(2), S434-S437

[33] Aragon-Sanabria, V., Kim, G., Randolph, L., Jiang, H., Reynolds, J., Webb, B., . . . Dong, C. (n.d.). TQM13 CAR T-cells enhance delivery of clickable biodegradable fluorescent nanoparticles in brain tumors.

Academic Vita

Hali A. Jiang

hali.jiang97@gmail.com

EDUCATION

The Pennsylvania State University, University Park, PA
Schreyer Honors College
Bachelor of Science in Biomedical Engineering
Minor in Psychology

WORK EXPERIENCE

Merck Manufacturing Science and Technology Intern *May '18- August '18*
West Point, Pennsylvania

- Designed, developed, and conducted a protocol to study particulate formation in oncology biologic admixture dilutions of lyophilized and liquid product
- Developed a surrogate formulation to match physical properties to a high viscosity biologic (mAb) commercial product for use in machinability and developmental studies

RESEARCH EXPERIENCE

Cellular Biomechanics Lab Undergraduate Research Assistant
University Park, Pennsylvania *September '16 – May '19*

- Developing analytical lab skills under Dr. Cheng Dong's direction
- Conducting experiments to examine the interactions between epithelial and immune cells to create a method of cancer treatment delivery that can bypass the blood-brain barrier
- Collaborating with Dr. Lian on CAR T immunotherapy receptor targets for glioblastoma

NSF Funded Summer Research Internship
University Park, Pennsylvania *June - August '17*

- Assessed the feasibility of utilizing primary lymphocytes to carry nanoparticles targeting brain tumors
- Characterized potential effects of lymphocytes and TNF-α on the blood-brain barrier by conducting in vitro experiments using cell monolayers

INTERNATIONAL EXPERIENCE

National University of Singapore Mechanical Engineering Product Design Program
Singapore, Singapore *May - June '16*

- Collaborated with students from the National University of Singapore, Brigham Young University, and Penn State University
- Attended lectures detailing the process of product design
- Designed a functioning prototype to improve worker safety and efficiency of rubbish collection from Singaporean apartment chutes

LEADERSHIP & INVOLVEMENT

Facilitator, Penn State WEP Study Groups *January '17 – January '19*

- Lead weekly study groups reviewing calculus and vector analysis material
- Form relationships with group members acting as a mentor

Penn State Schreyer for Women *January '17 – January '19*

- Served as service chair on the founding executive board establishing the vision of the club
- Contacted organizations to establish relationships and organized community service events

Past Involvements:

- Family Relations THON Chair, Blue and White Society
- Envoy, Penn State Sophomore Ambassador Team
- Mail/Pen Pal Chair, THON Rules and Regulations Committee

SOFTWARE & SKILLS

MATLAB
SOLIDWORKS
Fluent in Mandarin Chinese
COMSOL
Mammalian Cell Culture